Observation Data and 3D Map-based Radio Environment Estimation for Drone Wireless Communications

Shota Yamada*, Takeo Fujii*, Katsuya Suto† and Koya Sato‡
*† Advanced Wireless and Communication Research Center (AWCC), The University of Electro-Communications
† Graduate School of Information and Engineering, The University of Electro-Communications
‡ Artificial Intelligence eXploration Research Center, The University of Electro-Communications
1–5–1 Chofugaoka, Chofu, Tokyo 182–8585, Japan
Emails: {s.yamada, fujii}@awcc.uec.ac.jp, k.suto@uec.ac.jp, k_sato@ieee.org

***Abstract*—Toward next-generation mobile communication systems such as beyond 5G and 6G, non-terrestrial networks (NTNs) have attracted much attention as they extend the coverage of wireless communication services. In NTNs, drones have multiple roles, such as delivery service and transportation, while providing communication services. Therefore, radio environment estimation in three-dimensional (3D) space is crucial for stable drone operations. However, the impact of the surrounding structures and terrain on the radio environment is not well investigated. In this paper, we propose a method to estimate the received power in the direction of altitude by fusing observed signal data and a 3D map that records the geometry of terrain and structures. The proposed method divides the estimation area into a line-of-sight (LOS) altitude and a non-line-of-sight (NLOS) altitude, the estimation values for each range, and then integrates them to obtain the overall estimation values. Through the simulation using the actual measurement dataset, it is demonstrated that the proposed method outperforms the conventional empirical propagation model, i.e., Hata model.**

***Index Terms*—Radio Propagation Model, Radio Map, Non-Terrestrial Network, Drone, 3D Map**

I. Introduction

In recent years, wireless communication technology has become an essential and integral part of modern society as it continues to advance. It is expected that the use cases for mobile communications will continue to expand in the future. It is predicted that by 2028, global mobile traffic worldwide will reach approximately 325 exabytes per month, which is nearly four times the amount compared to 2022, due to the further increase in the number of communication devices [1]. To accommodate communication in various terminals such as smartphones and Internet of Things (IoT) devices, the 5th Generation mobile communication system (5G) has been implemented in Japan in 2020. Research and development are underway for the next-generation communication systems known as Beyond 5G/6G. In Beyond 5G, the goal is to enhance the characteristics of 5G while also aiming for improvements in autonomy, scalability, and reliability. As part of the efforts to improve scalability, expanding the coverage area of communication is being planned. While mobile communications have primarily focused on terrestrial networks, there is growing interest in extending the scope to include non-terrestrial networks (NTNs) that cover airspace and even outer space. In the context of Non-Terrestrial Networks (NTN), drones are expected to have various applications, such as serving as temporary base stations or providing a new means of transportation, like flying cars [2].

Drones are piloted by radio control and data transmission is performed using wireless communications. To enable proper network switching and route planning for drones in the airspace, it is crucial to have an accurate understanding of the surrounding radio environment. Conventional methods for understanding the radio environment use empirical propagation models such as the Okumura-Hata model [3] and the ITU-R P.1411 site-general model [4]. These models can predict the propagation loss at the applied location by inputting the surrounding environment of the propagation path, such as the distance between the transmitter and receiver, carrier frequency, and antenna height. However, shadowing and multipath fading, which are the effects of shielding by buildings and other structures, are not identified, so large prediction errors may occur in urban environments where buildings and other structures are densely located.

There is a ray tracing method [5] that enables the accurate assessment of the radio environment, including local attenuation involving shadowing effects. In this method, radio waves are treated as rays, and the reflection, diffraction, and transmission of these rays by surrounding 3D structures are geometrically traced to determine propagation losses. The availability of 3D models of terrains, structures, and objects such as 3D maps has made it easier to obtain them, thus expanding the potential for the use of ray tracing. Indeed, in [6], propagation analysis for drones is conducted using ray tracing. However, accurately modeling the material and surface roughness of structures can be challenging, and the computational requirements can be significant. As a result, it may not be suitable for immediate radio environment estimation. Therefore, the use of radio maps has been attracting attention in recent years as a computationally inexpensive but accurate method of estimating the radio environment [7]. The radio

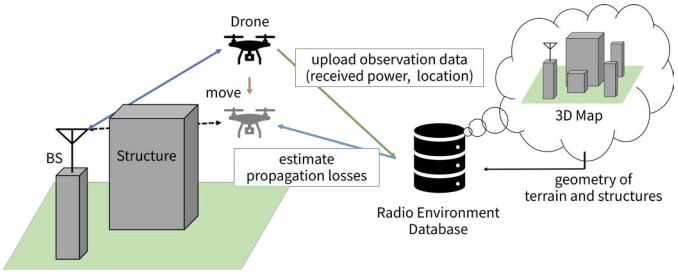

Fig. 1. Illustration of system model.

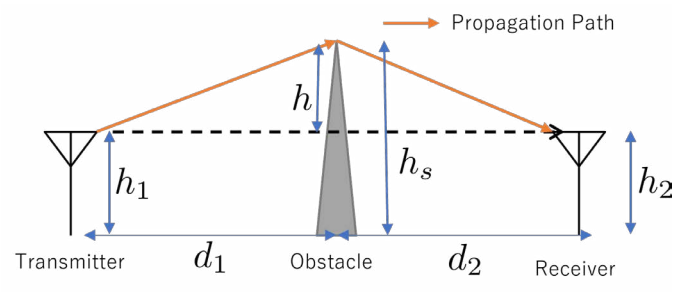

Fig. 2. Knife-edge diffraction.

map is a map that stores the average received power for each location mesh that divides the geographic space into a grid pattern and is constructed based on actual measurements. On the other hand, radio maps are based on the accumulation of radio environments observed by radio wave sensors and mobile terminals, and basically cover a two-dimensional area near the ground surface. Although it is theoretically possible to create a radio map in 3D space by defining each position mesh in 3D space and recording the observed values, it is difficult to record the observed values for the entire range of actual operation because the terminals in 3D space are limited. Therefore, it is necessary to interpolate and extrapolate the estimated received power at each location mesh from a limited set of observations. In this paper, we investigate and evaluate a method for predicting the received power in the height direction from a limited number of observations. In [8], an interference power estimation method is investigated, which utilizes a 2D radio map on the ground surface and 3D map information consisting of terrain and structural data. This study considers scenarios where observations beyond the ground surface are available. To further improve the estimation accuracy, this study proposes a method that derives diffraction losses in propagation paths from a set of observations obtained within a range including the airspace, three-dimensional maps, and parameters between transmitter and receiver points. By utilizing the difference in diffraction losses, this method estimates the received power at arbitrary positions and altitudes.

The structure of this paper is as follows. Section II describes the system model, and Section III explains the details of the estimation method. Section IV describes the observation experiment for the evaluation of the estimation method, and Section V describes the evaluation of the estimation accuracy when using the observation data. Finally, we conclude this paper in Section VI.

II. System Model

A. Assumed database environment

The system model assumed in this paper is shown in Fig. 1. The drone connects to a ground base station (BS) and records actual observation data consisting of received signal power, location information, and Physical Cell ID (PCI) of the connecting base station. The drone uploads the actual observation data recorded by the drone to the database server. Then the database server utilizes the uploaded actual observation data to derive diffraction loss values based on the 3D map information. By performing propagation estimation, it predicts the connectivity quality between drones and base stations. With the predicted results of the connectivity quality, drones can make use of network switching and efficient route selection.

B. Knife-edge diffraction model

In the above system model, existing diffraction loss models are utilized to perform diffraction calculations for arbitrary receiver locations. When obstacles such as buildings and terrain exist between the transmitting and receiving antennas, as shown in Fig. 2, the propagation path is obstructed, resulting in diffraction. In the Recommendation ITU-R P.526 [9], the diffraction loss $J(\nu)$ [dB], is formulated using the knife-edge diffraction loss model, as expressed in

$$J(\nu) = 6.9 + 20\log\left(\sqrt{(\nu - 0.1)^2 + 1} + \nu - 0.1\right). \quad (1)$$

Note that ν is a diffraction parameter that indicates the degree of shielding and is defined by

$$\nu = \Delta h \sqrt{\frac{2}{\lambda}\left(\frac{1}{d_1} + \frac{1}{d_2}\right)}, \quad (2)$$

where λ [m] is the wavelength, Δh [m] is the height from the line connecting the transmitting and receiving points to the knife-edge apex, h [m] is the height from the ground surface of the obstacle, h_{TX} [m] and h_{RX} [m] are the height of the transmitting and receiving points, respectively. d_1 [m] is the distance from the transmitting point to the obstacle, and d_2 [m] is the distance from the obstacle to the receiving point, respectively. Considering the equivalent earth radius Ka, h is expressed as

$$h = -\frac{h_{\mathrm{TX}} d_2 + h_{\mathrm{RX}} d_1}{d_1 + d_2} + \frac{d_1 d_2}{2Ka} + h. \quad (3)$$

Let the equivalent earth radius coefficient $K = 4/3$ and the earth radius be $a = 6370 \times 10^3$ [m].

C. 3D map

The 3D map information is constructed through methods such as satellite positioning, and it includes terrain information with elevation as well as the recorded height and shape of 3D structures such as buildings [10]. These 3D models, which

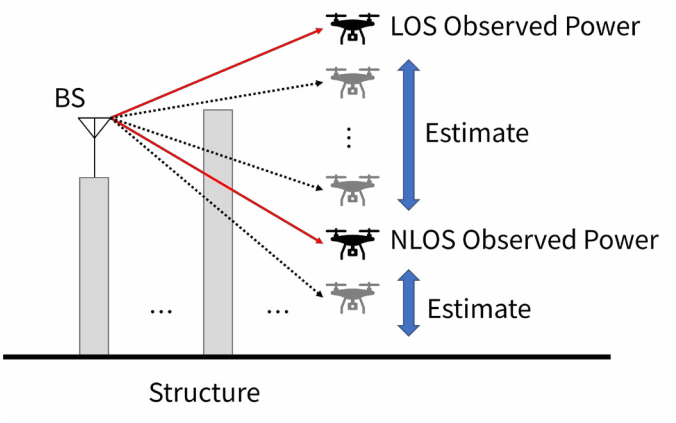

Fig. 3. Illustration of assumed scenario.

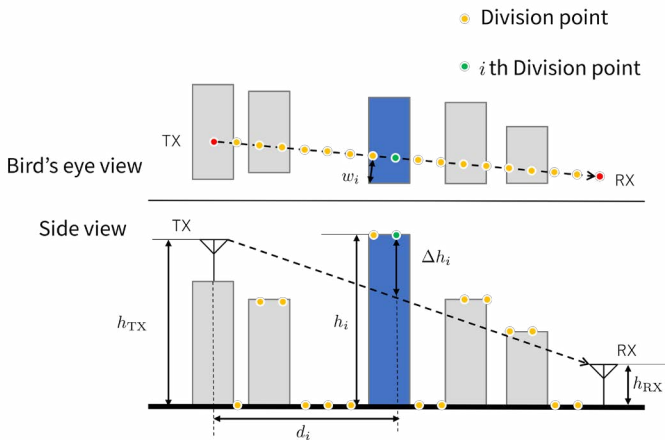

Fig. 4. Main structure and parameters.

represent actual urban environments, are utilized in urban planning and other related fields. They aim to simulate and accurately depict the urban landscape for various applications and analyses. The structural information is recorded in vector data formats such as Geoshape, enabling the retrieval of the height and vertex coordinates of each structure. The terrain information is recorded in raster data formats such as GeoTIFF, allowing for the extraction of elevation at any desired coordinates.

III. Proposed Method

A. Assumed scenario

The proposed method assumes a situation in which observed received power can be recorded by a drone equipped with observation devices. Based on the premise that the observed received power can be obtained in both Line-Of-Sight (LOS) and Non-Line-Of-Sight (NLOS) areas within the estimated region, the propagation estimation is performed using the following information:

- Set of observed received power values and the position and height of the receiver
- 3D map containing terrain and structural information
- Position and height of the transmitting base station.

The estimation is performed considering each two-dimensional position with respect to the altitude direction. The assumed environment is illustrated in Fig. 3.

B. Estimation procedure

(1) Search for the main structure between the receiving and transmitting locations.

To derive the diffraction loss values between the transmitting and receiving points, the structure that most obstructs the propagation path is detected from the 3D map as the main structure. First, the path between the transmitter and the receiver locations is divided at regular intervals. The path profile is acquired at each division point. The path profile consists of the height h_i [m] of the structure at the division point, the horizontal distance d_i [m] from the transmission point to the division point, and the coordinates of the vertices of the structure at the division point. From the acquired path profile, search for the point where the diffraction parameter ν_i is the largest in the knife-edge diffraction loss, as described in the Eq. (1) in Section II,

$$\nu_i = \min(\Delta h_{i_{\mathrm{g}}}, w_i)\sqrt{\frac{2}{\lambda}\left(\frac{1}{d_i}+\frac{1}{d-d_i}\right)}. \tag{4}$$

where $\Delta h_{i_{\mathrm{g}}}$ [m] is the height from the line connecting the transmitter point and the receiver point above ground to the split point, and is expressed by applying the equivalent radius of the earth as follows

$$\Delta h_{i_{\mathrm{g}}} = -\frac{h_{\mathrm{TX}}(d-d_i)+h_{\mathrm{RX_g}}(d_i)}{d}+\frac{d(d-d_i)}{2Ka}+h_i, \tag{5}$$

where h_{TX} [m] is the height including elevation of the transmitting point, $h_{\mathrm{RX_g}}$ [m] is the antenna height above the receiving point ground, d [m] is the horizontal distance from the transmitting point to the receiving point. Also, w_i [m] is the width from the straight line connecting the transmitting and receiving points to the structure edge, and the minimum distance from each vertex of the structure is adopted. The structure with the largest ν_i obtained in the search is set as the main structure that mainly shields the propagation path. Fig. 4 shows an overview of the main structure and parameters.

(2) Calculate the knife-edge diffraction loss due to the main structure for each receiving antenna altitude.

Derive the diffraction parameters in $J(\nu_h)$ and $J(\nu_w)$ for the knife-edge diffraction losses on the top and side edges of the main structure at each antenna height at the estimated location according to

$$\nu_{\mathrm{h}} = \Delta h_{i_{\mathrm{a}}}\sqrt{\frac{2}{\lambda}\left(\frac{1}{d_i}+\frac{1}{d-d_i}\right)}, \tag{6}$$

$$\nu_{\mathrm{w}} = w_i\sqrt{\frac{2}{\lambda}\left(\frac{1}{d_i}+\frac{1}{d-d_i}\right)}, \tag{7}$$

where $\Delta h_{i_{\mathrm{a}}}$ is obtained by replacing $h_{\mathrm{RX_g}}$ in equation (5) with the antenna height at the receiving point $h_{\mathrm{RX_a}}$.

(3) Distinguish the LOS or NLOS between the transmitting and receiving points.
If either ν_{h} or ν_{w} is less than or equal to -0.78, the environment between the transmitting and receiving points is judged to be LOS. Otherwise, the environment is judged to be NLOS.

(4) Derive diffraction loss values for each environment.
In a LOS environment, the loss value L [dB] is set to 0, assuming that there is a direct wave arrival from the transmitting point to the receiving point. In the case of an NLOS environment, the loss value L [dB] is equivalent to the average loss value $J_{\mathrm{av}}(\nu)$ [dB] when both diffracted waves from the top and side of the structure arrive,

$$J_{\mathrm{av}}(\nu) = -10\log\left(\frac{1}{10^{\frac{J(\nu_{\mathrm{h}})}{10}}} + \frac{1}{10^{\frac{J(\nu_{\mathrm{w}})}{10}}}\right). \tag{8}$$

In a prospective environment, the estimated received power value $\hat{P}_{\mathrm{est}}[\mathrm{dBm}]$ is estimated as equivalent to the received power value P_{meas} [dBm] obtained in the same environment,

$$\hat{P}_{\mathrm{est}} = P_{\mathrm{meas}}. \tag{9}$$

In an NLOS environment, when the receiver moves vertically and the antenna height changes, the difference in received power values is the difference in diffraction loss value J_{av} at each antenna height. The received power estimate $\hat{P}_{\mathrm{est}}$ [m] at height h_{est} [m] is derived from the following formula.

$$\hat{P}_{\mathrm{est}} = P_{\mathrm{meas}} - \left(J_{\mathrm{av}}(\nu_{\mathrm{est}}) - J_{\mathrm{av}}(\nu_{\mathrm{meas}})\right), \tag{10}$$

where P_{meas} [dBm] is the observed received power value $J_{\mathrm{av}}(\nu_{\mathrm{est}})\,[\mathrm{dB}]$ is the average diffraction loss at the height where the estimated value is obtained, $J_{\mathrm{av}}(\nu_{\mathrm{meas}})\,[\mathrm{dB}]$ is the average diffraction loss at the height of the observed value.

Finally, the estimated received power values for the LOS and NLOS environments are combined. To prevent overestimation of the diffraction loss value, the estimated power in the NLOS environment is set as the upper limit of the estimated power in the LOS environment, assuming that the power in the NLOS environment increases with antenna height to the power value in the LOS environment.

IV. Measurement Campaign

To evaluate the usefulness of the proposed method, a drone experiment was conducted in February 2023 in the north side of the University of Electro-Communications West Building W-2 (hereafter referred to as W2), an environment equivalent to an urban area, to observe the radio environment above the building. The target of measurement was the LTE signal of a commercial base station with a center frequency of 2120 [MHz]. The signals were observed using an area evaluation instrument (PCTEL IBflex), and the RSRP (Reference Signal Received Power) for each PCI was recorded. Fig. 5 shows a bird's-eye view of the relationship between the target base stations and the observation points in the measurement environment.

Fig. 6 shows the north-side view of W2. W2 is 64 [m] wide, 8 stories high, and 28.8 [m] high. Radio wave observations

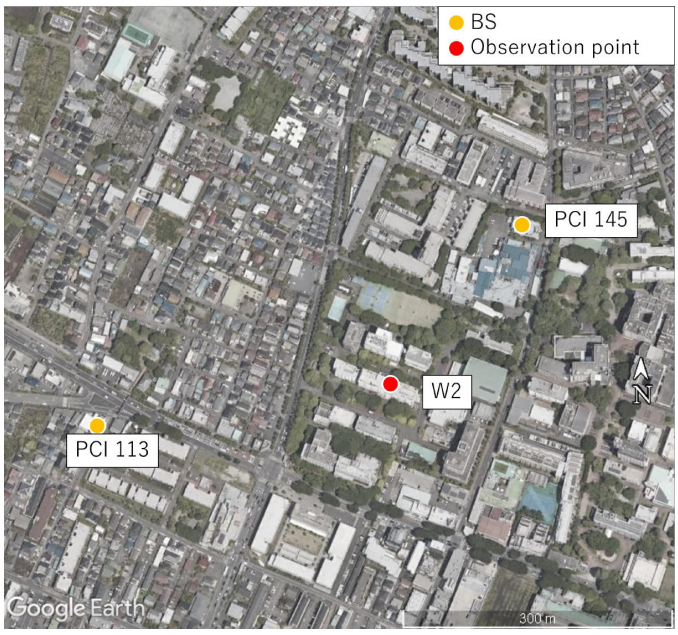

Fig. 5. Observation situation.

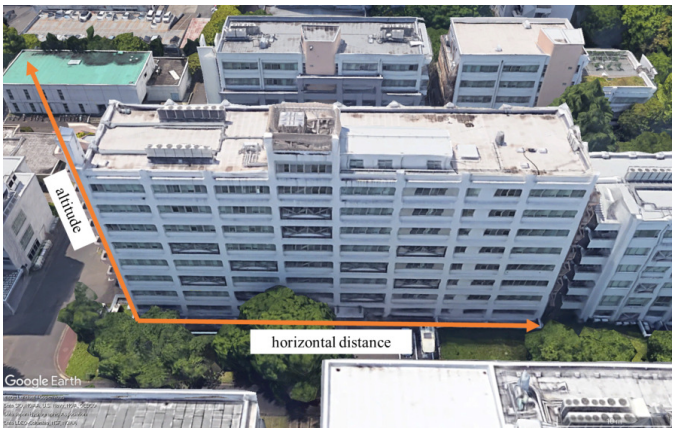

Fig. 6. Side view of W2.

were made by hovering at multiple points at intervals of 3 [m] from the wall for about 30 [s] each. The flight points were spaced 8 [m] apart in the horizontal direction, in the altitude direction up to the 8th floor, and 3 [m] apart above the rooftop, up to an altitude of 46.8 [m]. In addition, observations were made at altitudes of 50 [m] and 100 [m]. The observation position was recorded by linking the positional information observed by the GPS onboard the drone with the time axis. The parameters are shown in Table I. The information on the base stations is shown in Table II.

Based on the observed values from the area evaluation instrument, a radio map was constructed for each PCI by calculating the average received power at each flight point, taking into account the altitude direction. The results are shown in Fig. 7.

The horizontal distance of the radio map is 0 [m] at the

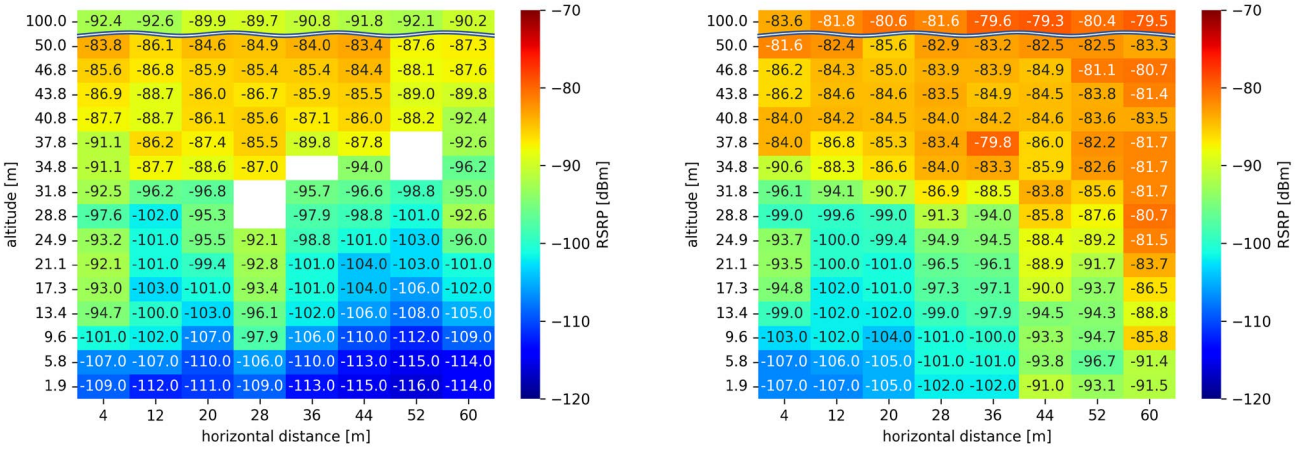

(a) PCI113 (b) PCI145

Fig. 7. Received power maps.

TABLE I
MEASUREMENT PARAMETERS.

Date of observation	2023/02/12
Observation site	Building W-2
Number of observation points	8×16 grids
Frequency band	LTE Band1 (2120[MHz])
Observation duration	about 30[s]
GPS	mounted on drone
Terminal	PCTEL IBflex
Observation cycle	about 0.25[s]

TABLE II
BASE STATION CONFIGURATIONS.

PCI	113	145
latitude	35.65709	35.65902
longitude	139.53768	139.54283
antenna height[m]	15	15

west end, and the distance to the east is shown. Blank grids in the radio map correspond to the areas where no observation data were obtained. The received signal power of both PCI113 and PCI145 tends to increase as the altitude increases. In both cases, the influence of the LOS environment is significant at altitudes above 31.8 [m], which is the range above the rooftop, and the received power is higher. PCI113's received power value drops at an altitude of 100 [m]. The base station of PCI145 is located in the northeast direction from W2, and the received power increases on the east side due to the influence of the smaller distance between the transmitting and receiving points.

V. ESTIMATION ACCURACY ANALYSIS

In this paper, we use root mean squared error (RMSE) to evaluate the estimation accuracy for the entire estimation area; in our model, the RMSE can be defined as

$$\mathrm{RMSE} = \sqrt{\frac{1}{n}\sum_{i=1}^{n}\left(\bar{P}_{\mathrm{meas},i} - \hat{P}_{\mathrm{est},i}\right)^2}, \tag{11}$$

where n is the number of observation grids, $\bar{P}_{\mathrm{meas},i}$ [dBm] is the average observed received power on grid i and $\hat{P}_{\mathrm{est},i}$ [dBm] is the estimated received power for grid i. The distribution of RMSE between observed received power and estimated received power was investigated in each of the following situations:

- In each column in the estimation area, one observed received power is obtained at random. Then the proposed method was used without distinguishing LOS or NLOS.
- Randomly obtained observed received power and the difference of the extended Hata model [11] is used.
- The observed data in the LOS environment and NLOS environment are randomly obtained in each column of the estimation area and the proposed method was used with distinguishing LOS or NLOS.

The distributions of RMSE between estimated and measured values except for the grid where the observed values were obtained when repeated 1000 times are shown in Fig. 8. In Fig. 8, 'Mixed LOS/NLOS' is the result without the distinguishing LOS, 'Ext. Hata' is the result using the extended Hata model, and 'Proposed' is the result applying the proposed method with the distinguishing LOS and area segmentation. Each distribution is represented by a box plot. The central orange line represents the median, and the upper and lower whiskers represent the maximum and minimum values, respectively. Outliers are not defined in this context. The median and mean of each RMSE are shown in Table III.

The results show that the RMSE is minimized for both PCI113 and PCI145 when the proposed method with lookahead determination is used. For PCI113, the average RMSE was improved by approximately 3.23 [dB], and for PCI145,

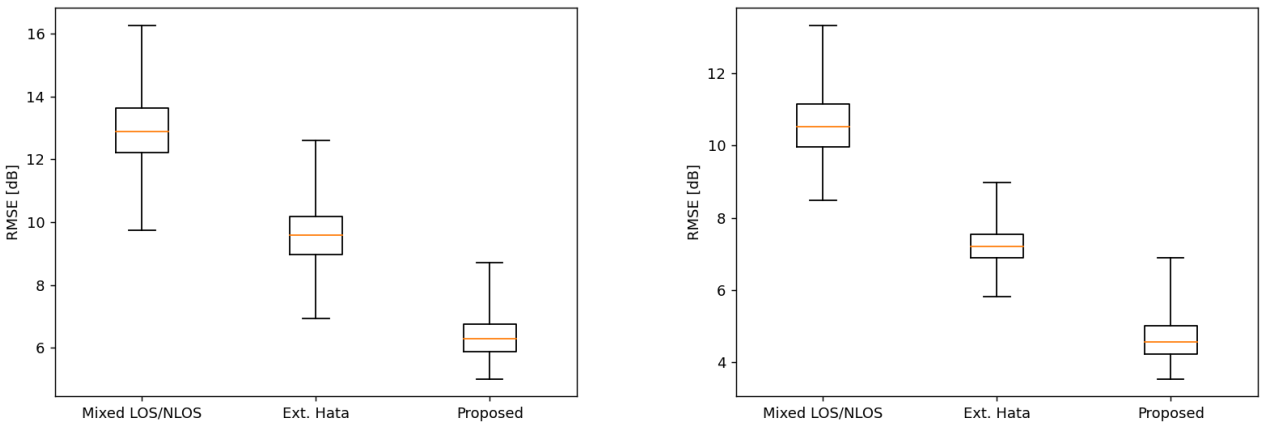

(a) PCI113 (b) PCI145

Fig. 8. RMSE distributions.

TABLE III
RMSE PERFORMANCES.

	PCI113		
	Mixed LOS/NLOS	Ext. Hata	Proposed
mean [dB]	12.94	9.60	6.37
median [dB]	12.90	9.60	6.29
	PCI145		
	Mixed LOS/NLOS	Ext. Hata	Proposed
mean [dB]	10.55	7.23	4.68
median [dB]	10.51	7.22	4.56

by approximately 2.55 [dB], compared to the case using the extended Hata model. On the other hand, one random observation was obtained for each column of the estimation area, and the RMSE was approximately 10 [dB] or more for both PCI 113 and 145 when we operated the proposed method without distinguishing LOS. This is due to an overestimation of the loss value when extrapolating the estimated value of the outlook environment from the observed value of the unobserved environment alone.

VI. CONCLUSION

In this paper, we have proposed a method for estimating the radio environment in the direction of altitude by combining actual observations in the sky and 3D map information. Experimental results show that the proposed method provides a more accurate propagation estimation than the existing radio propagation model, which estimates propagation by the difference of loss values in the extended Hata model when the observed values are available for both the LOS and NLOS environments.

The method proposed in this paper currently targets only the up and down directions and does not take into account the effects of beam patterns in a LOS environment and the presence of multiple structures that significantly obstruct the propagation path. In the future, we plan to develop a method that can estimate more three-dimentionally, including diagonally and horizontally, taking into account the beam pattern and multiple structures.

ACKNOWLEDGMENT

These research results were obtained from the commissioned research(No.02601) by National Institute of Information and Communications Technology (NICT), Japan.

REFERENCES

[1] Ericsson, “Ericsson mobility report, November 2022,” Ericsson, Stockholm, Sweden. Nov. 2022. [Online]. Available: https://www.ericsson.com/4ae28d/assets/local/reports-papers/mobility-report/documents/2022/ericsson-mobility-report-november-2022_compressed.pdf(Accessed: Jan. 22, 2023)

[2] S. Ansari, A. Taha, K. Dashtipour, Y. Sambo, Q. H. Abbasi, and M. A. Imran, “Urban air mobility—a 6G use case?,” *Frontiers in Communications and Networks*, vol. 2, 2021.

[3] M. Hata, “Empirical formula for propagation loss in land mobile radio services,” in *IEEE Trans. on Veh., Technol.*, vol. 29, no. 3, pp. 317–325, Aug. 1980.

[4] Rec. ITU-R P.1411-11, “Propagation data and prediction methods for the planning of short-range outdoor radiocommunication systems and radio local area networks in the frequency range 300 MHz to 100 GHz,” ITU-R, Sept. 2021.

[5] Z. Yun and M. F. Iskander, ”Ray tracing for radio propagation modeling: principles and applications,” in *IEEE Access*, vol. 3, pp. 1089-1100, 2015.

[6] M. U. Sheikh, K. Ruttik, N. Saba, E. Mutafungwa, R. Jäntti and J. Hämäläinen, “Analysis of drone propagation with ray tracing from Sub-6 GHz upto terahertz frequencies in a real world urban environment,” ICOIN 2021, Jeju Island, Korea (South), 2021, pp. 169-174.

[7] Y. Zeng and X. Xu, “Toward Environment-Aware 6G Communications via Channel Knowledge Map,” in *IEEE Wireless Communications*, vol. 28, no. 3, pp. 84-91, June 2021.

[8] S. Miyamoto, S. Yamada and T. Fujii, “Height pattern estimation method using the combination of radio map and 3D map for spectrum sharing,” ICOIN 2023, Bangkok, Thailand, Jan. 2023.

[9] Rec. ITU-R P.526-15, “Propagation by diffraction,” ITU-R, Oct. 2019

[10] T. Tadono, J. Takaku, K. Tsutsui, F. Oda and H. Nagai, “Status of ‘ALOS World 3D (AW3D)’ global DSM generation,” IGARSS 2015, Milan, Italy, 2015, pp. 3822-3825.

[11] Rec. ITU-R SM.2028-2, “Monte Carlo simulation methodology for the use in sharing and compatibility studies between different radio services or systems,” ITU-R, June 2017.